Journal of Alloys and Compounds 509 (2011) 751–757

Contents lists available at ScienceDirect

Journal of Alloys and Compounds

journal homepage: www.elsevier.com/locate/jallcom

Destabilization of $LiBH_4$ by $(Ce, La)(Cl, F)_3$ for hydrogen storage

Bang Jie Zhang[a], Bin Hong Liu[a,*], Zhou Peng Li[b]

[a] Department of Materials Science and Engineering, Zhejiang University, Hangzhou 310027, PR China
[b] Department of Chemical Engineering, Zhejiang University, Hangzhou 310027, PR China

ARTICLE INFO

Article history:
Received 19 July 2010
Received in revised form 6 September 2010
Accepted 8 September 2010
Available online 22 September 2010

Keywords:
Hydrogen storage material
Borohydride
Halides of rare earth
Dehydrogenation
Reversibility

ABSTRACT

The mixtures of $LiBH_4$ with halides of Ce or La in a molar ratio of 3:1 were investigated to explore their hydrogen storage properties. The ball milling of $LiBH_4$ with chloride of Ce or La yielded $Ce(BH_4)_3$ and $La(BH_4)_3$, while fluoride of Ce or La did not react with $LiBH_4$ during extended ball milling at room temperature. The dehydrogenation temperatures of the ball-milled mixtures were reduced to 220–320 °C, which were much lower than that of pure $LiBH_4$. The diborane emission during hydrogen release was observed at a low level. The dehydrogenation temperature is found to be affected by the composition of rare earth halides, but less influenced by ball milling time. The endothermic dehydrogenation reactions produced lithium halides, hydrides and borides of the corresponding rare earth element. Moreover, the $LiBH_4 + 1/3(Ce, La)(Cl, F)_3$ showed partial reversibility through the formation of an unknown borohydride, allowing for a potential hydrogen storage system.

1. Introduction

Hydrogen is regarded as an ideal energy carrier due to its high energy density and environmental-friendly nature. However, hydrogen has to be stored efficiently and safely in versatile applications. Currently, extensive effort is being devoted to exploring new hydrogen storage materials with high gravimetric and volumetric hydrogen densities [1–8]. Metal borohydrides are one group of compounds with the highest hydrogen capacities and thus considered as candidates for hydrogen storage. $LiBH_4$, as the representative, contains 18.4 wt.% hydrogen and is thus attracting considerable attentions as a promising material for hydrogen storage [3–4,6–24].

The reversible hydrogen storage of $LiBH_4$ could be achieved through following reaction.

$$LiBH_4 = LiH + B + 3/2H_2 \quad (1)$$

However, reversible hydrogen storage of $LiBH_4$ requires harsh conditions. For example, hydrogen desorption from $LiBH_4$ takes place at temperature as high as 400 °C, while the re-hydrogenation needs 600 °C and 35 MPa [3]. Therefore, it is necessary to destabilize $LiBH_4$ and enable hydrogen desorption and absorption at mild conditions. Some additives were found to be effective in destabilizing $LiBH_4$. Zuttel et al. [3,4] reported that $LiBH_4$ with SiO_2 could release hydrogen below 300 °C. Vajo et al. [6,7] found that the combination of $LiBH_4$ and MgH_2 could effectively destabilize the system, resulting in reversible hydrogen storage at reduced temperatures. Other additives like Al [9,10], carbon materials [11,12], TiO_2, V_2O_5 [13,14] and halides such as $TiCl_3$, TiF_3 and ZnF_2 [15] could also reduce the dehydrogenation temperature of $LiBH_4$.

Among various additives, transition metal halides are one group of destabilizing agents for $LiBH_4$. Halides of Ti [15] and Zr [17], chlorides of Mn [23], chlorides of Fe, Co, Ni [24], halides of Zn [15,17] have been added to reduce the dehydrogenation temperature of $LiBH_4$. The main reason for the destabilization is due to the instability of corresponding transition metal borohydrides [19]. Nakamori et al. [16] suggested that the cation M^{n+} in $M(BH_4)_n$ plays an important role in deciding the stability of borohydride. The thermal desorption temperature of $M(BH_4)_n$ is inversely proportional to the Pauling electronegativity of the metal M. As the electronagativities of transition metals are larger than that of Li, the stabilities of their borohydrides will be much lower than that of $LiBH_4$, enabling dehydrogenation at lower temperatures. However, the additions of these transition metal halides often result in irreversibility of the systems, which is undesirable for developing hydrogen storage materials.

Recently, it was reported by Gennari et al. [22] that $Ce(BH_4)_3$ was synthesized through ball milling the mixture of $LiBH_4$ and $CeCl_3$, and desorbed hydrogen at low temperatures. Moreover, they found that the decomposed sample could absorb some hydrogen. However, they did not report further the re-hydrogenation process. This result inspires an expectation for a potentially reversible hydrogen storage system. Therefore in this study, we investigated the dehydrogenation and re-hydrogenation process of the

* Corresponding author. Tel.: +86 571 87951770; fax: +86 571 87951770.
E-mail address: liubh@zju.edu.cn (B.H. Liu).

0925-8388/$ – see front matter © 2010 Elsevier B.V. All rights reserved.
doi:10.1016/j.jallcom.2010.09.066

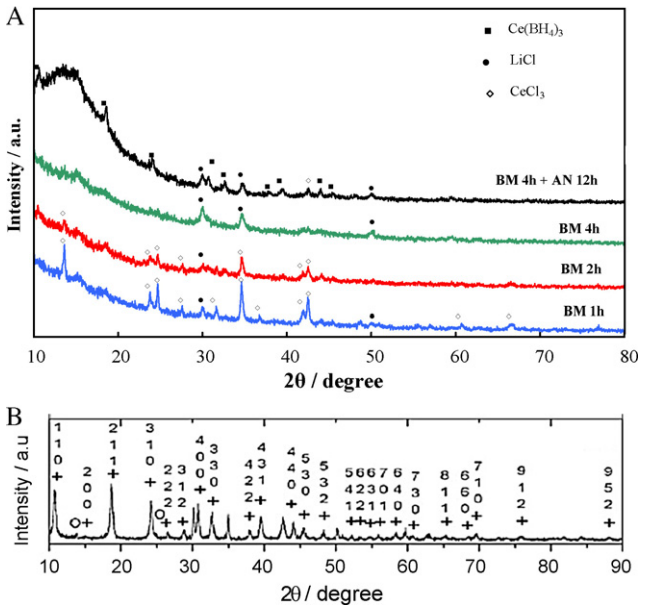

Fig. 1. (A) Our XRD analysis results of the ball milled $LiBH_4 + 1/3CeCl_3$ mixtures (BM: ball milling, AN: annealing). (B) XRD result of $Ce(BH_4)_3$ reported by Gennari et al. [22].

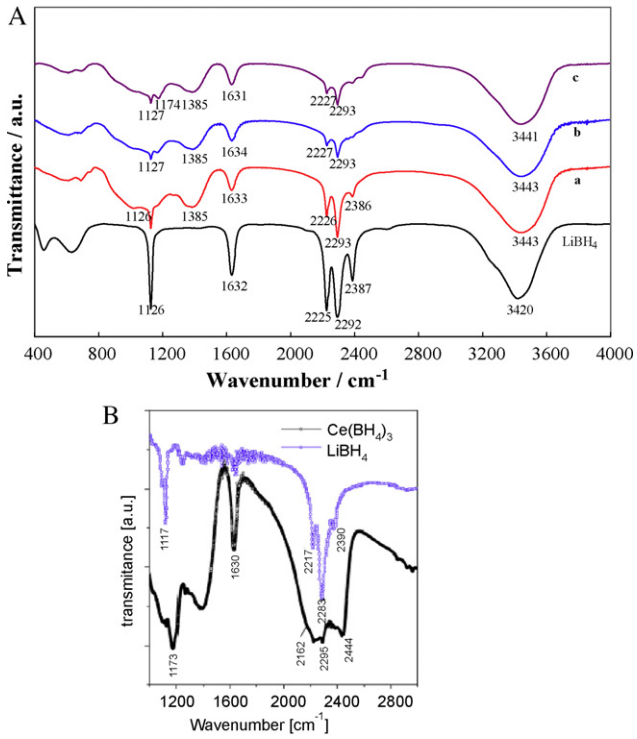

Fig. 2. (A) Our FTIR spectra of $LiBH_4$ and the ball milled $LiBH_4 + 1/3CeCl_3$ mixtures (a) ball milled for 2 h; (b) ball milled for 4 h; and (c) ball milled for 4 h and annealed at 100 °C for 12 h. (B) FTIR results reported by Gennari et al. [22].

ball milled $LiBH_4 + 1/3(Ce, La)(Cl, F)_3$ in some detail to explore reversible hydrogen storage systems. The effects of rare earth metal and halide element on dehydriding and rehydriding properties of $LiBH_4 + 1/3(Ce, La)(Cl, F)_3$ were also studied.

2. Experimental

$LiBH_4$ (95% purity) and LaF_3 (99.9% purity) were purchased from J&K Chemicals. Other halides $CeCl_3 \cdot 7H_2O$, $LaCl_3 \cdot 7H_2O$ and CeF_3 of analytical grade were commercially available from Sinopharm Chemical Reagent Co. Ltds. Anhydrous $CeCl_3$ and $LaCl_3$ were prepared by dehydrating $CeCl_3 \cdot 7H_2O$, $LaCl_3 \cdot 7H_2O$ at 190 °C for 24 h under vacuum. The samples of $LiBH_4 + 1/3(Ce, La)(Cl, F)_3$ were ball milled on a planetary mill at a speed of 500 rpm for different periods. The stainless steel vessel for ball milling was of 100 ml and the ball to sample weight ratio was 40:1. The dehydrogenation and hydrogenation properties of the mixtures were examined in a Sieverts apparatus. The reactor was first evacuated to 10^{-3} Torr and then heated at a rate of 2 °C min^{-1} from room temperature to 450 °C or 600 °C. The hydrogen desorption amount was then determined according to pressure rise in the system and the hydrogen desorption weight percentage was calculated with respect to the weight of $LiBH_4$ instead of the total weight of the mixture. The hydrogenation was performed by holding the dehydrogenated sample at elevated temperatures under a hydrogen pressure of 10.0 MPa.

X-ray diffraction analyses were performed on a PANalytical X'Pert PRO using the CuK_α radiation. A sample stand covered by glass was specially prepared to keep the samples from air exposure during sample transferring. The sample window was covered by a layer of transparent plastic film that demonstrated no specific peaks in XRD patterns. The Fourier transform infrared spectrometry (FTIR) analyses were carried out on a Bruker Tensor 27. About 1 mg of the sample was first mixed with 100 mg KBr in a mortar in the glovebox, and then the mixture was pressed into a pellet under 10 MPa. The pellet was then introduced into the cell and the test was finished within 1 min. The samples were examined within the wavenumber range of 4000–400 cm^{-1}. The coupled DSC-TG-MS analyses were conducted on a Netzsch STA449F3 equipped with a Netzsch Q430C mass spectrometer. During the measurements, the samples were heated at a rate of 10 °C min^{-1} under high purity argon with a purge rate of 50 ml min^{-1}.

All the samples were handled in a glove box under high-purity argon atmosphere to avoid air contamination. O_2 and H_2O in the glove box were kept below 1 ppm.

3. Results and discussion

3.1. Formation of $Ce(BH_4)_3$ and $La(BH_4)_3$

The mixture of $LiBH_4 + 1/3CeCl_3$ was ball milled at 500 rpm for different time. Fig. 1 gives the XRD patterns of the ball milled mixtures. The newly appeared peaks in the 1 h ball milled sample could be assigned to LiCl, indicating the occurrence of a reaction during the ball milling process. With the increase of ball milling time, the peak intensities from $CeCl_3$ were reduced, while those from LiCl were increased. After 4 h ball milling, only the peaks from LiCl were detected. Assuming that other reaction products might be present in a very dispersed or amorphous form so that they were not detectable by XRD analysis, we annealed the 4 h ball milled sample at 100 °C for 12 h. As a result, a new set of peaks became clearly visible in the XRD profiles of the annealed sample. The pattern of the new substance resembles with the one reported by Gennari et al. for $Ce(BH_4)_3$ [22], suggesting that $Ce(BH_4)_3$ crystallized after the annealing treatment. The structure of $Ce(BH_4)_3$ is characterized as a cubic structure by Gennari et al. with $a = 11.640$ Å. Our XRD results yield a lattice constant of $a = 11.643$ Å, which is very close to Gennari et al.'s.

The FTIR spectra also gave evidences supporting the formation of $Ce(BH_4)_3$. As shown in Fig. 2, $LiBH_4$ demonstrates three characteristic B–H stretching bands of 2225, 2292 and 2387 cm^{-1} as well as a B–H bending band at 1126 cm^{-1}. With the formation of $Ce(BH_4)_3$, these characteristic bands remain but with some subtle changes, indicating the presence of a new borohydride. For example, the stretching bands of 2225, 2292, 2387 cm^{-1} are not shifted but the 2387 cm^{-1} band becomes weak. A large shoulder appears around the band of 1126 cm^{-1}. Also a new broad band at 1385 cm^{-1} is observed that is not contributed either by the halides in reactants nor products nor KBr, enabling us to assign this band to $Ce(BH_4)_3$.

Similar results were obtained for the mixture of $LiBH_4 + 1/3LaCl_3$. As shown in Fig. 3, the ball milling induced a reaction between $LiBH_4$ and $LaCl_3$ because LiCl was detected in the 16 h ball milled mixture. Like $Ce(BH_4)_3$, $La(BH_4)_3$ was not detectable in the as-received ball milled mixture. But after the annealing at 100 °C for 12 h, the sample clearly revealed the presence of a new phase with a similar pattern as that of $Ce(BH_4)_3$. It indicates that $La(BH_4)_3$ was synthesized with a cubic structure of $a = 11.695$ Å.

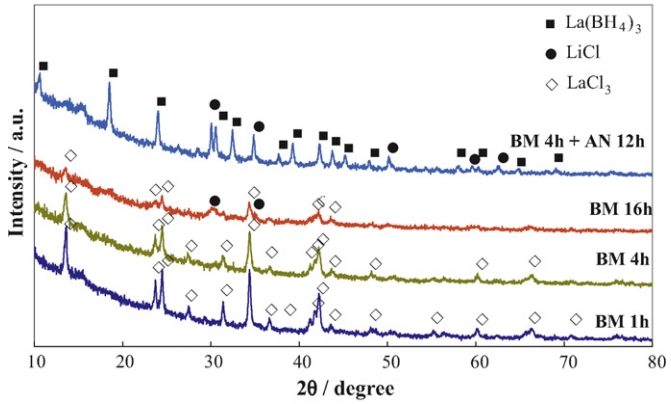

Fig. 3. XRD patterns of the ball milled $LiBH_4 + 1/3LaCl_3$ mixtures (BM: ball milling, AN: annealing).

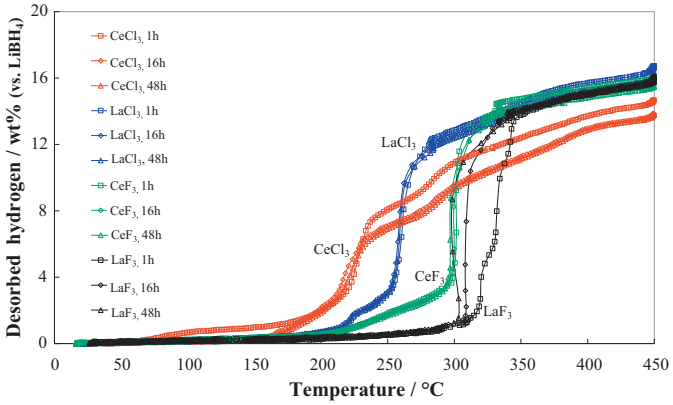

Fig. 5. Dehydrogenation characteristics of the ball milled $LiBH_4 + 1/3(Ce, La)(Cl, F)_3$ mixtures with different ball milling time (heating rate during dehydrogenation: 2 °C min^{-1}).

The FTIR study provided additional evidence for the formation $La(BH_4)_3$. As shown in Fig. 4, the FTIR spectrum of $La(BH_4)_3$ is almost identical to that of $Ce(BH_4)_3$, suggesting that both have very similar structures.

In order to examine the effects of halide element on the synthesis of borohydride of Ce or La, we also used CeF_3 and LaF_3 as the precursors. However, the fluoride of Ce or La was not as reactive as the chlorides. No LiF was detected in the mixtures even when the ball milling time was extended to 48 h. The FTIR spectra did not demonstrate apparent changes from $LiBH_4$ to $Ce(BH_4)_3$ or $La(BH_4)_3$ either. These results indicate that the reaction between $LiBH_4$ and fluorides did not occur at the present conditions.

3.2. Dehydrogenation characteristics of $LiBH_4 + 1/3(Ce, La)(Cl, F)_3$ mixtures

Fig. 5 shows the dehydrogenation characteristics of the ball-milled $LiBH_4 + 1/3(Ce, La)(Cl, F)_3$ mixtures, from which several effects could be observed. First, the additions of these halides into $LiBH_4$ reduced dehydrogenation temperature significantly. For pure $LiBH_4$, the main dehydrogenation temperature is well above 400 °C [3], while it was decreased to 220–320 °C for the mixtures. It suggests that $LiBH_4$ is destabilized by the addition of the halides. Second, the additions of Ce halides resulted in lower dehydrogenation temperatures than corresponding La halides. Third, the mixtures containing chlorides revealed lower dehydrogenation temperatures than those with fluorides. As a result, the $CeCl_3$ addition yielded the lowest dehydrogenation temperature of 220–280 °C, while the mixture with LaF_3 showed the highest one of 320 °C. Finally, the ball milling time had little effect in modifying dehydrogenation properties except for the LaF_3 addition.

The XRD profiles shown in Fig. 6 reveal that the mixture decomposed into several phases after dehydrogenation. In the sample heated to 250 °C, only LiCl was visible. When the mixture was heated to 450 °C, CeH_2 appeared as well and for the mixture heated to 600 °C, CoB_6 was clearly identified. Therefore, it could be concluded that the solid products of the dehydrogenated mixture were LiCl, CeH_2 and CeB_6. Gennari et al. [22] did not directly observe CeB_6 in the decomposed $Ce(BH_4)_3$ through their XRD studies but they presumed the formation of CoB_6 based on the hydrogen amount obtained in the experiment and a thermodynamic consideration. In this study, our direct observation of CoB_6 verifies their assumption.

A DSC-TG-MS coupled analysis was performed to further elucidate the dehydrogenation reaction of the ball milled mixtures. The DSC profiles in Fig. 7(A) reveal that the 1 h milled $LiBH_4 + 1/3CeCl_3$ mixture had some residual $LiBH_4$ as the endothermic peak at 105 °C is attributed to the structural change of $LiBH_4$. The absence of this peak for the 16 h and 48 h milled samples indicates that $LiBH_4$ had been fully transformed to $Ce(BH_4)_3$. As the temperature rose up, two dehydrogenation peaks were observed at about 220 °C and 280 °C respectively, both of which were endothermic in the DSC profile. It can be noted that three samples demonstrated similar dehydrogenation behaviors regardless of their differences in $Ce(BH_4)_3$ abundance, suggesting that the dehydrogenation characteristics were not highly dependent on the formation of $Ce(BH_4)_3$. The MS analysis detected a low level of B_2H_6 during the second dehydrogenation peak, suggesting that a small amount of boron was lost during hydrogen release.

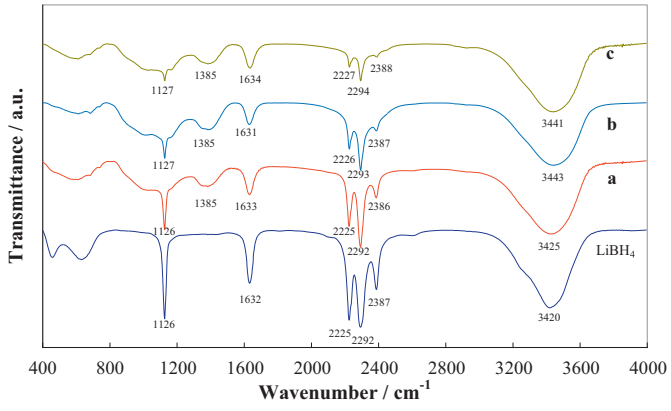

Fig. 4. FTIR spectra of $LiBH_4$ and the ball milled $LiBH_4 + 1/3LaCl_3$ mixtures: (a) ball milled for 4 h; (b) ball milled for 16 h; (c) ball milled for 4 h and annealed at 100 °C for 12 h.

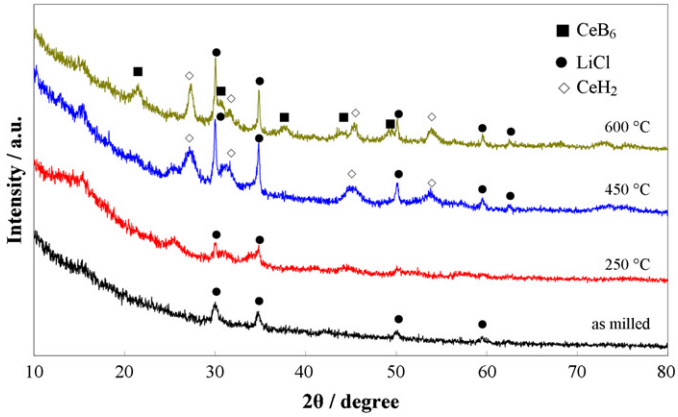

Fig. 6. XRD profiles of $LiBH_4 + 1/3CeCl_3$ mixtures after dehydrogenation to different temperatures.

Based on the above analysis results, it could be deduced that the dehydrogenation reaction proceeds as the following reaction:

$$LiBH_4 + 1/3CeCl_3 \rightarrow LiCl + 1/3Ce(BH_4)_3$$
$$\rightarrow LiCl + 1/6CeH_2 + 1/6CeB_6 + 11/6H_2 \quad (2)$$

The standard enthalpy change of the above reaction is calculated to be 23.2 kJ mol H_2^{-1} at 298 K. The observed heat effects accompanying with hydrogen release in the DSC experiments of the 1 h, 16 h and 48 h-milled $LiBH_4 + 1/3CeCl_3$ mixtures were −36.0, −24.8 and −22.7 kJ mol H_2^{-1} respectively (negative values mean endothermic effects). The differences in heat effect are ascribed to their different states after ball milling.

The hydrogen desorption capacity of the above reaction is 3.53 wt.% with respect to the total weight of the mixture, and 16.8 wt.% on basis of $LiBH_4$. In this work, the hydrogen desorption capacity at 450 °C obtained by the volumetric method was 14.6 wt.% on basis of $LiBH_4$ and 3.05 wt.% vs. the total weight.

Compared with $Ce(BH_4)_3$, $La(BH_4)_3$ decomposed at somewhat higher temperature of 270 °C as shown in Fig. 7(B). Although there exists one small hydrogen desorption peak at around 220 °C, the major dehydrogenation temperature is at 270 °C. As LiCl, LaH_2, LaB_6 were identified in the XRD profile of the 600 °C dehydrogenated mixture, the following reaction could be deduced:

$$LiBH_4 + 1/3LaCl_3 \rightarrow LiCl + 1/3La(BH_4)_3$$
$$\rightarrow LiCl + 1/6LaH_2 + 1/6LaB_6 + 11/6H_2 \quad (3)$$

Although $Ce(BH_4)_3$ or $La(BH_4)_3$ was not achieved through ball milling the mixture of $LiBH_4$ with the fluoride of Ce or La, the addition of CeF_3 and LaF_3 caused significant decreases in dehydrogenation temperature. As shown in Fig. 7(C), both 48 h milled mixtures of $LiBH_4 + 1/3(Ce, La)F_3$ demonstrate clearly the structural change at 105 °C and melting peak at 260 °C of $LiBH_4$, indicating that $LiBH_4$ remained unreacted and $Ce(BH_4)_3$ and $La(BH_4)_3$ were not formed even at higher temperatures. It thus suggests that the dehydrogenation reaction occurred directly between $LiBH_4$ and the fluorides. By analogy to $LiBH_4$+1/3(Ce, La)Cl_3, the dehydrogenation of $LiBH_4 + 1/3(Ce, La)F_3$ might proceed as follows:

$$LiBH_4 + 1/3CeF_3 \rightarrow LiF + 1/6CeH_2 + 1/6CeB_6 + 11/6H_2 \quad (4)$$
$$LiBH_4 + 1/3LaF_3 \rightarrow LiF + 1/6LaH_2 + 1/6LaB_6 + 11/6H_2 \quad (5)$$

The $LiBH_4 + 1/3(Ce, La)(Cl, F)_3$ mixtures demonstrated similarities and differences in several features. For example, they resembled to each other in following aspects: First, the dehydrogenation reactions are all endothermic and their standard enthalpy changes are much smaller than that of $LiBH_4$ dehydrogenation, as

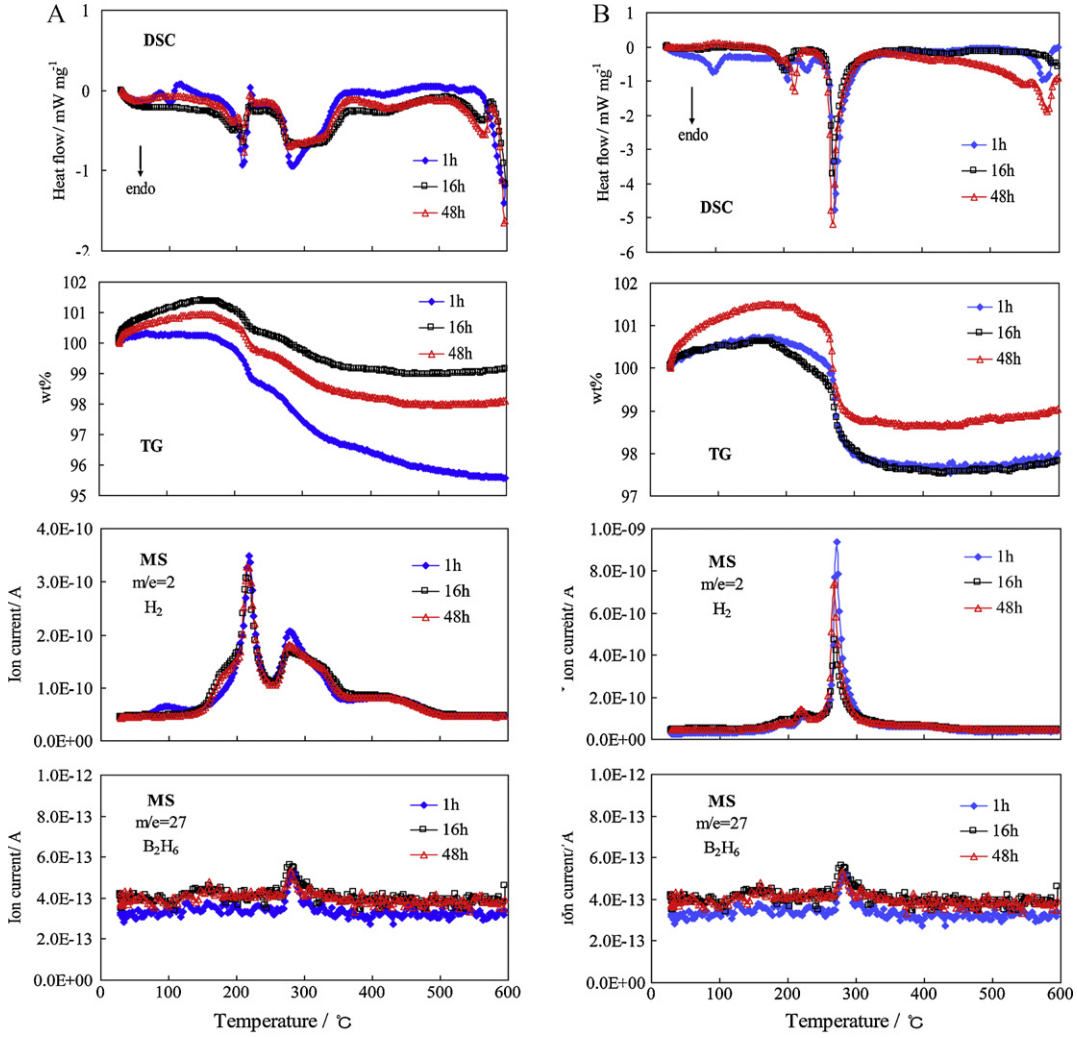

Fig. 7. (A) DSC-TG-MS analysis results showing the dehydrogenation characteristics of the ball milled $LiBH_4 + 1/3CeCl_3$ mixtures with different ball milling time (heating rate: 10 °C min^{-1}). (B) DSC-TG-MS analysis results for the ball milled $LiBH_4 + 1/3LaCl_3$ mixtures with different ball milling time (heating rate: 10 °C min^{-1}). (C) DSC-TG-MS analysis results showing the dehydrogenation characteristics of the ball milled $LiBH_4 + 1/3(Ce, La)F_3$ mixtures with different ball milling time (heating rate: 10 °C min^{-1}).

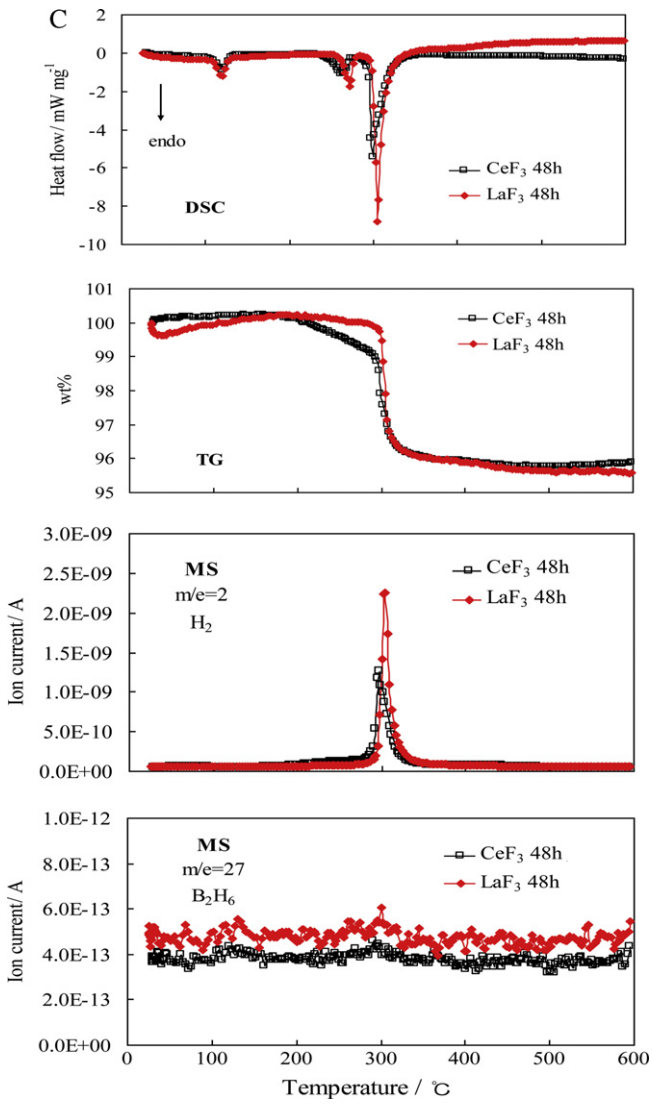

Fig. 7. (*Continued*).

shown in Table 1. Second, the decomposition produced hydrides and borides of rare earth element. Third, only small amounts of B_2H_6 were emitted with hydrogen. Compared with the dehydrogenation reaction of $LiBH_4$ destabilized by other additives [15,20,24], the B_2H_6 emission in this study was relatively at a low level. The main reason may be attributed to the formation of CeB_6 or LaB_6. Considering the atomic ratio of 1:6 in CeB_6 and LaB_6, boron was supposed to be tightly bonded by Ce or La in the solid phase through the formation of CeB_6 or LaB_6 (the standard formation enthalpies of CeB_6, LaB_6 and B_2H_6 are −351.5, −104.2 and 35.6 kJ mol^{-1} respectively), thus preventing the formation of B_2H_6.

The differences demonstrated by these additions include the formation of $Ce(BH_4)_3$ and $La(BH_4)_3$ using chlorides but the negative result using fluorides. Also the dehydrogenation temperatures were varied. Table 1 lists the calculated thermodynamic data for the dehydrogenation reactions. It can be concluded that the thermodynamic factors may only partially account for the difference between chlorides and fluorides, as well as the differences between Ce and La halides.

The ball milling time in most cases had little effect on dehydrogenation properties of the milled mixtures, indicating that the formation and abundance of $Ce(BH_4)_3$ or $La(BH_4)_3$ in the mixture did not significantly influence the dehydrogenation process. But in the case of LaF_3 addition, the ball milling time showed positive effects in enhancing the dehydrogenation revealed in Fig. 5, implying the reaction was kinetically impeded.

3.3. Re-hydrogenation properties

The hydriding characteristics of the dehydrogenated $LiBH_4 + 1/3(Ce, La)Cl_3$ composites were investigated to explore the reversibility of the system. The dehydrogenated mixtures were held at 350 °C or 450 °C for 24 h under 10 MPa H_2 for re-hydrogenation and then the dehydrogenation was carried out. As shown in Fig. 8 the 350 °C and 450 °C hydrogenated sample released about 3.5 wt.% and 4.4 wt.% hydrogen. They correspond to 25% and 32% of the original hydrogen release amount of the as-milled mixture, indicating that only partial reversibility was achieved. Further experiments showed that this part of hydrogen capacity was reversible, but gradually decreased to 2.4 wt.% at 5th hydriding–dehydriding cycle.

The XRD patterns in Fig. 9 display phase transitions during the dehydrogenation and hydrogenation process. After the re-hydrogenation, the presence of some un-identified peaks suggests the formation of a new phase. Its disappearance after the second

Table 1
Thermodynamic calculations for the reactions.

Reactions	ΔH° (298 K, kJ mol H_2^{-1})	ΔG° (298 K, kJ mol H_2^{-1})
$LiBH_4 = LiH + B + 3/2H_2$	66.9	37.8
$LiBH_4 + 1/3CeCl_3 = LiCl + 1/6CeH_2 + 1/6CeB_6 + 11/6H_2$	23.2	−8.2
$LiBH_4 + 1/3CeF_3 = LiF + 1/6CeH_2 + 1/6CeB_6 + 11/6H_2$	25.6	−4.1
$LiBH_4 + 1/3LaCl_3 = LiCl + 1/6LaH_2 + 1/6LaB_6 + 11/6H_2$	48.2	15.9
$LiBH_4 + 1/3LaF_3 = LiF + 1/6LaH_2 + 1/6LaB_6 + 11/6H_2$	49.3	34.4

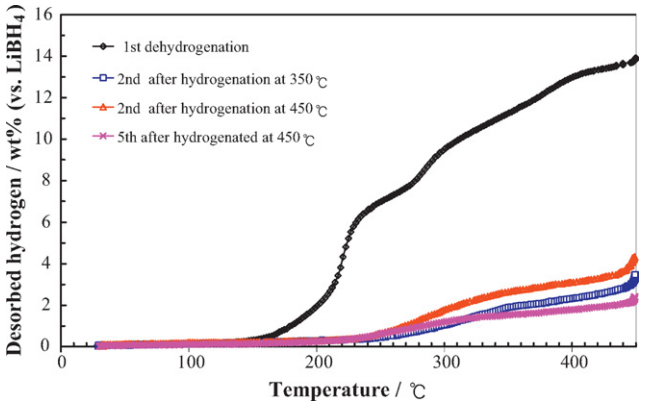

Fig. 8. Comparison of dehydrogenation characteristics for the as-milled and hydrogenated mixtures with the original composition of $LiBH_4 + 1/3CeCl_3$ (dehydrogenation conditions: heating rate 2 °C min^{-1}; hydrogenation conditions: holding at 350 °C or 450 °C under 10.0 MPa H_2 for 24 h).

dehydrogenation implies that the new phase accounts for the partial reversibility of the composite. From the FTIR analysis result given in Fig. 10, the hydrogenated sample shows the characteristic bands of B–H at 1126 cm^{-1} and 2225, 2292, 2387, 2476 cm^{-1}, which are analogous to those of $LiBH_4$ rather than $Ce(BH_4)_3$. As the un-identified phase can also be found traceably in the first dehydrogenated sample shown in Fig. 9, it is highly possible that the new phase in the hydrogenated sample was an intermediate formed during the multi-step dehydrogenation of $Ce(BH_4)_3$. However, the exact characterization of the new phase requires more sophisticated approaches.

Similar results were obtained when $LiBH_4 + 1/3LaCl_3$ was investigated. The hydrogenation was also carried out at 350 °C or 450 °C under 10 MPa H_2 for 24 h. The 350 °C hydrogenated sample desorbed 3.3 wt.% H_2 and the 450 °C one released 3.7 wt.% H_2 with respect to the original $LiBH_4$ amount. The XRD analysis did not detect the presence of new phases after hydrogen absorption but the FTIR result revealed the characteristic bands of B–H for the

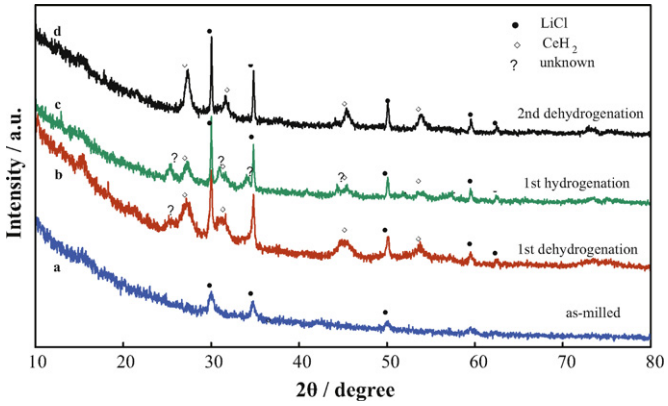

Fig. 9. XRD patterns of the $LiBH_4 + 1/3CeCl_3$ mixtures in different states: (a) as milled mixture; (b) 1st dehydrogenation at 2 °C min^{-1} to 450 °C; (c) 1st re-hydrogenation at 450 °C, 10.0 MPa H_2 for 24 h; (d) 2nd dehydrogenation at 2 °C min^{-1} to 450 °C.

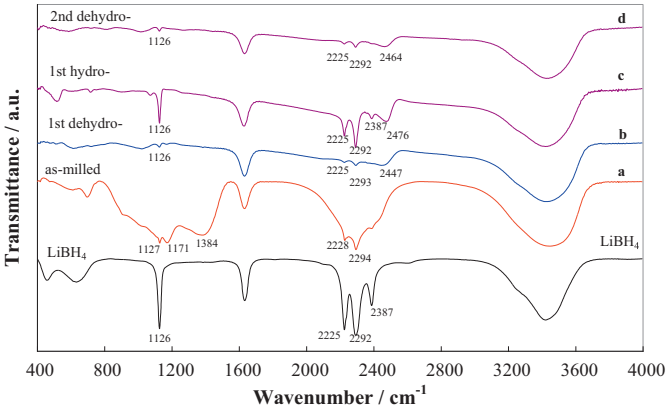

Fig. 10. FTIR spectra of pure $LiBH_4$ and $LiBH_4 + 1/3CeCl_3$ mixtures in different states: (a) as milled mixture; (b) 1st dehydrogenation at 2 °C min^{-1} to 450 °C; (c) 1st re-hydrogenation at 450 °C, 10.0 MPa H_2 for 24 h; (d) 2nd dehydrogenation at 2 °C min^{-1} to 450 °C.

hydrogenated sample, indicating the formation of a BH_4^--like compound.

The above results show some encouraging phenomena for a reversible hydrogen storage system. However, further investigation is required to clarify the hydrogenation process and enhance the reversibility of the system through effective catalysis.

4. Conclusions

The composites of $LiBH_4 + 1/3(Ce, La)(Cl, F)_3$ were investigated to develop new hydrogen storage systems with high hydrogen storage capacity. $Ce(BH_4)_3$ and $La(BH_4)_3$ were obtained through the ball milling of $LiBH_4$ with the chlorides, while the fluorides did not react with $LiBH_4$ during ball milling at room temperature. The ball milled mixtures demonstrated dehydrogenation temperatures around 220–320 °C, which were much lower than that of pure $LiBH_4$. The dehydrogenation temperature was affected by the composition of rare earth halides, while it was less influenced by the ball milling time. As a result, the addition of $CeCl_3$ resulted in the lowest dehydrogenation temperature, while LaF_3 addition yielded the highest one. The dehydrogenation produced lithium halide, hydride and boride of the corresponding rare earth element. The $LiBH_4 + 1/3(Ce, La)(Cl, F)_3$ showed partial reversibility through the formation of an unknown borohydride.

Acknowledgements

This work is financially supported by the National Natural Science foundation of No. 50971114 and National 973 program of No. 2010CB631304 as well as the Hi-tech projects of Zhejiang Province of No. 2009C21011.

References

[1] B. Bogdanovic, M. Schwickardi, J. Alloys Compd. 253–254 (1997) 1–9.
[2] P. Chen, Z.T. Xiong, J.Z. Luo, J.Y. Lin, K.L. Tan, Nature 420 (2002) 303–304.

[3] A. Zuttel, S. Rentsch, P. Fischer, P. Wenger, P. Sudan, Ph. Mauron, Ch. Emmenegger, J. Alloys Compd. 356–357 (2003) 515–520.
[4] A. Zuttel, P. Wenger, S. Rentsch, P. Sudan, Ph. Mauron, Ch. Emmenegger, J. Power Sources 118 (2003) 1–7.
[5] W.F. Luo, J. Alloys Compd. 381 (2004) 284–287.
[6] J.J. Vajo, S.L. Skeith, F. Mertens, J. Phys. Chem. B 109 (2005) 3719–3722.
[7] J.J. Vajo, G.L. Olson, Scripta Mater. 56 (2007) 829–834.
[8] S. Orimo, Y. Nakamori, J.R. Eliseo, A. Zuttel, C.M. Jensen, Chem. Rev. 107 (2007) 4111–4132.
[9] J. Yang, A. Sudik, C. Wolverton, J. Phys. Chem. C 111 (2007) 19134–19140.
[10] X.D. Kang, P. Wang, L.P. Ma, H.M. Cheng, Appl. Phys. A 89 (2007) 963–966.
[11] A.F. Gross, J.J. Vajo, S.L. Van Atta, G.L. Olson, J. Phys. Chem. C 112 (2008) 5651–5657.
[12] X.B. Yu, Z. Wu, Q.R. Chen, Z.L. Li, B.C. Weng, T.S. Huang, Appl. Phys. Lett. 90 (2007) 034106–034113.
[13] M. Au, A. Jurgensen, J. Phys. Chem. B 110 (2006) 7062–7067.
[14] M. Au, A. Jurgensen, K. Zeigler, J. Phys. Chem. B 110 (2006) 26482–26487.
[15] M. Au, A.R. Jurgensen, W.A. Spencer, D.L. Anton, F.E. Pinkerton, S.J. Hwang, C. Kim, R.C. Bowman, J. Phys. Chem. C 112 (2008) 18661–18671.
[16] Y. Nakamori, K. Miwa, A. Ninomiya, H.W. Li, N. Ohba, S. Towata, A. Zuttel, S. Orimo, Phys. Rev. B 74 (2006) 045126.
[17] H.W. Li, S. Orimo, Y. Nakamori, K. Miwa, N. Ohba, S. Towata, A. Zuttel, J. Alloys Compd. 446–447 (2007) 315–318.
[18] S. Orimo, Y. Nakamori, G. Kitahara, K. Miwa, N. Ohba, S. Towata, A. Zuttel, J. Alloys Compd. 404–406 (2005) 427–430.
[19] W. Grochala, P.P. Edwards, Chem. Rev. 104 (2004) 1283–1315.
[20] J. Kostka, W. Lohstroh, M. Fichtner, H. Hahn, J. Phys. Chem. C 111 (2007) 14026–14029.
[21] T. Sato, K. Miwa, Y. Nakamori, K. Ohoyama, H.W. Li, T. Noritake, M. Aoki, S. Towata, S. Orimo, Phys. Rev. B 77 (2008) 104114.
[22] F.C. Gennari, M.R. Esquivel, J. Alloys Compd. 485 (2009) L47–L51.
[23] R.A. Varin, L. Zbroniec, Int. J. Hydrogen Energy 35 (2010) 3588–3597.
[24] B.J. Zhang, B.H. Liu, Int. J. Hydrogen Energy 35 (2010) 7288–7294.